



HAL
open science

Structural lessons on bacterial secretins

Brice Barbat, Badreddine Douzi, Romé Voulhoux

► **To cite this version:**

Brice Barbat, Badreddine Douzi, Romé Voulhoux. Structural lessons on bacterial secretins. *Biochimie*, 2022, 205, pp.110-116. 10.1016/j.biochi.2022.08.019 . hal-03845257

HAL Id: hal-03845257

<https://hal.science/hal-03845257v1>

Submitted on 8 Dec 2022

HAL is a multi-disciplinary open access archive for the deposit and dissemination of scientific research documents, whether they are published or not. The documents may come from teaching and research institutions in France or abroad, or from public or private research centers.

L'archive ouverte pluridisciplinaire **HAL**, est destinée au dépôt et à la diffusion de documents scientifiques de niveau recherche, publiés ou non, émanant des établissements d'enseignement et de recherche français ou étrangers, des laboratoires publics ou privés.

1 **STRUCTURAL LESSONS ON BACTERIAL SECRETINS**

2

3 Brice Barbat¹, Badreddine Douzi² & Romé Voulhoux^{1*}

4

5 ¹LCB-UMR7283, CNRS, Aix Marseille Université, IMM, 13009 Marseille, France

6 ²Université de Lorraine, INRAE, DynAMic, 54000 Nancy, France

7

8 ***Correspondance :**

9 Email : voulhoux@imm.cnrs.fr

10 Postal address : LCB-UMR7283, CNRS, Aix Marseille Université, IMM, 31 Ch. J. Aiguier 13009

11 Marseille, France

12

13 **ABSTRACT**

14 To exchange and communicate with their surroundings, bacteria have evolved multiple active and
15 passive mechanisms for trans-envelope transport. Among the pore-forming complexes found in the
16 outer membrane of Gram-negative bacteria, secretins are distinctive homo-oligomeric channels
17 dedicated to the active translocation of voluminous structures such as folded proteins, assembled
18 fibers, virus particles or DNA. Members of the bacterial secretin family share a common cylinder-
19 shaped structure with a gated pore-forming part inserted in the outer membrane, and a periplasmic
20 channel connected to the inner membrane components of the corresponding nanomachine. In this
21 mini-review, we will present what recently determined 3D structures have told us about the
22 mechanisms of translocation through secretins of large substrates to the bacterial surface or in the
23 extracellular milieu.

24

25 **KEYWORDS**

26 bacterial secretin; beta-barrel; outer membrane; cryo-EM; structure-function

27

28 **HIGHLIGHTS**

29 - Secretins are the OM portal of the T2SS, T3SS, T4P and FPE systems

30 - Secretins form giant pores tailored to the secretion or assembly of large structures

31 - Secretins consist of a conserved OM C-module and a variable periplasmic N-module

32 - The channel formed by the C-module is occluded by a flexible central gate (CG)

33 - The N-module connect with the IM components of the respective systems

34 **1. Introduction**

35 Secretins were discovered in the 80's during the study of *Klebsiella oxytoca* outer membrane (OM)
36 constituents responsible for the export of folded pullulanase to the extracellular milieu [1]. Secretins
37 have been intensively since because of their unique ability to accommodate large folded exoproteins
38 and protein complexes in several bacterial transport nanomachines [2]. Due to their function, secretins
39 were thought for decades to form giant ring-shaped homo-oligomers in the OM [3-8], but their precise
40 atomic organization was deciphered only recently thanks to spectacular advances in cryo-electron
41 microscopy (cryo-EM) [9, 10]. This revealed extraordinary ternary and quaternary networks,
42 highlighting unsuspected structural determinants at the basis of functions hitherto observed but not
43 yet understood. In this mini-review, we will present how cryo-EM structural data shed light on the
44 architecture and function of bacterial secretins, and how structural determinants compartmentalize
45 and animate these giant pores embedded in the bacterial envelope.

46

47 **2. The bacterial secretin family**

48 The existence of a bacterial secretin family, first proposed by Genin and colleagues, comprised several
49 OM-associated proteins essential for the transport of macromolecules across bacterial membranes
50 [11]. Bacterial secretins are widely used by bacteria and even by mitochondria [12] in a variety of
51 transport systems specialized in the transit of large molecules across the OM. These range from
52 delivery of folded effectors by the Type 2 Secretion System (T2SS) to filament accommodation in the
53 case of the Type 3 Secretion System (T3SS) and Type 4 Pili (T4P) or phage release in the Filamentous
54 Phage Extrusion (FPE) system. Members of this family were historically defined by a highly conserved
55 C-terminal "secretin domain" which appeared to be the OM pore-forming domain [13], and a variety
56 of N-terminal domains, combinations of distinct modular domains connected via short linkers, whose
57 number depends on the transport machine [14]. For example, while the T2SS-secretin N-part is
58 composed of three repeated N3, N2 and N1 Ring-Building Motif (RBM) domains and a N0 TonB-
59 dependent transduction domain [15] possibly supplemented by a peptidoglycan binding SPOR domain
60 [16], the N-part of the other secretin types (T4P and FPE) are made up of N3 and N0 domains, optionally
61 completed by an internal N1 sub-domain for T3SS or two distal amidase N-terminal "AMIN" domains
62 for T4P [17]. Finally, the T2SS and T3SS secretins possess an additional extreme C-terminal S-domain,
63 the attachment site for a partner protein called pilotin, which assists secretin assembly and targeting
64 to the OM (see [18] for review).

65

66 **3. Cryo-EM reveals atomic 3D architecture of secretins**

67 3.1 Overall organization

68 Recent advances in the field of cryo-EM applied to isolated biological samples led to high-resolution
69 3D structures for at least one member of each bacterial secretin type (see Table 1 for an exhaustive
70 list of secretin near-atomic-resolution cryo-EM structures available). These structures – illustrative
71 examples are presented Figure 1 – revealed a bimodular organization with a well-defined OM C-
72 module, followed by a periplasmic variable N-module composed of several superposed ring-like
73 structures connected by short linkers. In most secretin structures, the C-module is resolved at a
74 resolution of 3-4 Å, whereas the resolution decreases over the N-module to become poor in the most
75 N-terminal N0 domain. It has been hypothesized that this results from the N0 domain high flexibility
76 in absence of its inner membrane (IM) interacting partner. This is in line with N0 high resolution in the
77 structure of the T2SS PulD secretin of *Klebsiella pneumoniae* copurified with its IM partner PulC [19].
78 The C-module found in all secretins has a structural organization into three domains, which could not

79 be predicted from the primary sequence. First, there is a giant double wall β -barrel with a closed
80 central gate (CG) that must open to allow the passage of the translocated structures. In some T2SS
81 secretins, the channel is capped by an additional top gate (TG). Second, we consider the N3 RBM-
82 domain, originally thought to be part of the N-domain, as part of the pore-forming C-module, which is
83 consistent with its structural role and conservation in secretins [20]. Finally, the extreme C-terminal S-
84 domain (specific of T2SS and T3SS-secretins) is composed of 2 α -helices that encircled the outer barrel.

85

86 3.2. Stoichiometry

87 The exact stoichiometry of secretins has always been and still is a matter of debate. Previous low-
88 resolution 3D structures suggested a homo-multimeric organization of 12, 14 or 15 subunits depending
89 on the type [14]. The recently reported high-resolution structures (listed in Table 1) are compatible
90 with these stoichiometries, at least for the C-modules. Either isolated or in complexes, T2SS, T3SS and
91 FPE secretins C-modules present a definite pentadecameric (C15) symmetry, whereas T4P secretins
92 primarily adopt a tetradecameric (C14) symmetry. Interestingly, different stoichiometries have
93 sometimes been reported for a given secretin C-module, e.g., 28 % of the *Escherichia coli* T2SS GspD
94 are hexadecameric (C16) [10], while 8 % of the *Pseudomonas aeruginosa* T4P PilQ adopt a C15
95 symmetry [21]. This variability does not appear to be restricted to secretin types, and it could therefore
96 constitute an additional adaptation to accommodate complex secretion/assembly processes.

97 The stoichiometry of N-modules is less well understood since their 3D structures are poorly,
98 or not at all, resolved, probably due to high intrinsic flexibility. This is regrettable because there is a
99 recurrent symmetry conflict for T3SS and T2SS secretins between C-modules and IM partners, which
100 present incompatible 15:24 and 15:12 stoichiometries, respectively [19, 22]. Recently, structures of
101 T3SS complexes including secretins and their IM partners indicate that the stoichiometry mismatch
102 could be resolved by the presence of additional secretin domains. In the case of *Salmonella enterica*
103 serovar Typhimurium T3SS, the presence of a sixteenth secretin subunit is clearly seen for the N0-N1
104 domains, leading to a compatible InvG₁₆:PrgH₂₄ interface with 8 additional PrgH subunits packing
105 around and under the β -sheet to reinforce the interface [22]. The addition of N0-N1 monomers in a
106 pentadecameric secretin was also observed for the *Shigella flexneri* T3SS secretin MxiD [23, 24]. For
107 T2SS, the interface region between the PulD N0 domain and its IM partner PulC is also puzzling with
108 an estimation of around 15 PulD-N0 for about 12 PulC-HR, leaving up to three PulD-N0 unoccupied
109 [19]. Independent work showed that the *P. aeruginosa* T2SS secretin XcpD (formerly XcpQ) adopts a
110 dodecameric (C12) conformation when purified without the C-module [25]. As proposed by Hay and
111 colleagues [26], such symmetry mismatch in T2SS secretins might be overcome by the displacement
112 of three XcpD N-modules away from the XcpC IM-partner-interface, thus leading to the formation of
113 the metastable C15:N12 arrangement. The overall stoichiometry of a given secretin might therefore
114 fluctuate, especially in its N-terminal part, to be compatible with the stoichiometry of its IM partner.
115 However, additional structural data is needed for a more complete understanding of this conundrum.

116

117 3.3. Charge distributions

118 While their structures are similar, the internal electrostatic characteristics of bacterial secretins vary
119 significantly from one secretin type to another but also within the same type (figure 2) [27, 28, 30].
120 The overall amount of charged amino acids is around 20 % depending on the secretin's type, but their
121 distribution on the quaternary structure is not homogeneous along the channel of each secretin. On
122 the structures available to date, it seems that the entry of the internal cavity in the N-terminal side has
123 a relatively positive charge, whereas in the N3 domain it turns to be relatively negative except for FPE

124 secretins. An important charge heterogeneity is found in a disordered loop in the N3-domain of
125 variable size, but neither its structural importance nor its functional role have been determined yet.
126 The variation of charge in the lower cavity could be important to stabilize the assembled filament inside
127 the secretin, or to allow the docking of the folded effector in T2SS, but these hypotheses have never
128 been investigated. Looking at the CG of T3SS secretins, we observe a predominant charge that is
129 opposite to the charge present on the wall of the upper cavity. Such charge distribution could allow
130 stabilization of the central gate once it is open considering that it stays open in this secretin when the
131 needle is assembled. The charge compatibility between the top of the CG and the β -barrel wall is not
132 seen in the T2SS, T4P and FPE secretins where these regions display relatively similar charge
133 distributions. In terms of dynamics, the presence of identical charges in these zones would lead to
134 electrostatic repulsion and therefore could allow rapid closing of the CG when the pseudopilus or pilus
135 is disassembled in the T2SS and T4P systems or when the phage particle has been secreted in the FPE
136 system. If we compare the different secretin types, the apical extremities show a wide range of global
137 charges (compare for example T4P and FPE secretins in figure 2), which could be an evolutionary
138 adaptation to their external environment.

139

140 **4. Secretin structures reveal discrete common and specific features**

141 4.1. The gated pore-forming domain

142 The pore-forming domain of bacterial secretins is highly conserved and form the OM portal through
143 which secreted substrates or translocated appendages transit to the cell surface. Recent cryo-EM data
144 revealed an atypical organization into a giant 56 to 64 stranded β -barrel, where each of the 14-16
145 subunits contributing a 4-stranded beta sheet (Table 1 and Figure 1). The high-resolution structures
146 also revealed an additional inner barrel formed by 4 β -strand per monomers, with the two upper
147 strands extending towards the center of the cavity, perpendicularly to the barrel wall, a structural
148 feature already suspected in many low-resolution structures of secretins [8, 20, 31]. The convergence
149 of their loops in the center of the cavity partially obturates the channel to form an orifice of variable
150 size, depending on the secretin type, but always too narrow to allow the transit of its corresponding
151 molecule. This observation agrees with previous studies of secretin channels pore size and
152 electrophysiology showing a pore with a small opening, akin to regular porins [7, 13, 32, 33]. This
153 structural feature separates the periplasmic chamber from the top cavity and is therefore named
154 central gate (CG) (Figure 1). The gating function of CG is supported by the fact that most of the
155 previously identified mutations in the FPE F1 phage secretin pIV, leading to gain of function growth on
156 maltopentaose, bile salt permeability or antibiotic sensibility [34], mapped to the CG [27]. CGs, most
157 often captured under closed conformation in isolated particles, must adopt an alternative open
158 conformation to allow the passage of the different structures secreted or assembled by secretins. Such
159 flexibility is comforted by the observation of a partially open CG and bile salt-sensitive phenotype for
160 the T2SS GspD_{G453A} variant, which harbors a glycine to alanine substitution in the central gate [10].
161 Sequence alignment of secretins show that glycine residues are systematically present at least at one
162 bending point of the CG β -strands. In accord with their high flexibility, these residues would allow the
163 rotation of the CG, which would flip upwards and come close to the β -barrel wall to accommodate the
164 secreted or assembled structure. Such opening mechanism has recently been confirmed by the 3D
165 structure of the T3SS secretin InvG in an open conformation with the needle assembled inside (Figure
166 1) [22]. Importantly, since CG modification not only results in leaky but also non-functional secretins,
167 passage through the CG is probably not a passive process [34]. Given the structural and functional
168 diversity of the molecules passing through this channel, it is not surprising that this diversity is reflected

169 in the CG primary sequences. It is indeed easy to imagine that to accommodate a static needle (T3SS),
170 a folded effector (T2SS), a highly dynamic pilus (T4P) or a bacteriophage (FPE), bacterial secretins must
171 display different CGs composition and dynamics. Interestingly, even among T2SS secretins, significant
172 sequence divergence exists in CGs that may reflect the exquisite substrate specificity existing between
173 different T2SS [10]. However, we still lack biochemical data on the interaction interfaces between CGs
174 and substrates to understand mechanistically how CGs function in different types of secretins.

175

176 4.2. The N3 RBM domain and its involvement in pore formation

177 Global observation of secretin 3D structures (Figure 1) indicates that the N3 domain, previously
178 associated by sequence homology to the periplasmic N-domains, constitutes the building blocks of the
179 C-module with the pore-forming domain. This structural reallocation of the N3 domain to the C-module
180 confirms previous functional data showing its requirement, in addition to the pore-forming domain,
181 for the assembly of a minimal secretin capable of forming a pore in the OM [13, 35]. The N3 RBM
182 domain has the propensity to form ring-like structures [36]. RBMs are also found outside of bacterial
183 secretins where they also play a central ring-building function, e.g., in the IM ring of the T3SS [37] or
184 the sporulation channel component SpoIIIAG [38]. Since T2SS secretins are independent of the β -barrel
185 assembly machinery (BAM), pre-folded in the periplasm and able to fold spontaneously *in vitro* [39], it
186 is tempting to speculate that the circular oligomerization of secretin C-module could be driven by the
187 ring-like self-assembly property of their RBM domain [37]. This notion is however challenged by a
188 recent structural study indicating that RBM most likely stabilise the oligomer rather than initiate its
189 oligomerization [40]. Nonetheless, RBM conservation in all secretins, as well as its essentiality for
190 oligomerization, support its reallocation as part of the upper C-module.

191

192 4.3. Secretin biogenesis and its scaffolding S domain

193 The different steps driving a protein initially synthesized in the cytoplasm to its final conformation and
194 location consist in overcoming multiple constraints. The secretins must not only travel to the OM but
195 also adopt a complex channel conformation, allowing the passage of large molecules without
196 perturbing bacterial envelope integrity. Their final destination being beyond the IM, the newly
197 synthesized pro-secretin monomer is taken over in the cytoplasm by the SecB chaperone to be
198 exported in the periplasm through the Sec translocon. Once exported, and after cleavage of the signal
199 sequence, secretin monomers are, most often, taken over by an escort protein called pilotin, which
200 will assist in their delivery and proper insertion into the OM [41]. Pilotin maintains the secretin in an
201 intermediate conformation compatible with its transport to the OM, preventing mis-localization
202 and/or premature oligomerization in the IM, which would be deleterious to cell integrity. Such
203 phenotypes have indeed been observed for T2SS and T3SS secretins in absence of their pilotins [42,
204 43]. Several types of mechanisms have been described for the transport of secretins from the
205 periplasm to the outer membrane [44]. The most common, used by most T2SS and T3SS secretins,
206 involves a lipidated pilotin, itself transported to the OM via the Lol pathway [45]. In this case, secretin
207 transport to the OM is independent of the BAM pathway [46] in agreement with its non- β -barreled
208 OM inserted domain [28] and its capacity to spontaneously insert in artificial vesicles [35]. Alternative
209 OM targeting for secretins have been described including Bam-dependent transport [47], involvement
210 of IM accessory proteins for T4P and T2SS secretins [41, 48], or no external assistance like for the self-
211 piloted T2SS HxcQ lipo-secretin [49]. Regarding secretin assembly, the existence of folded periplasmic
212 intermediates adopting different conformations prior to the OM insertion has been proposed [39].

213 Such process has been observed in many pore-forming proteins [50-52] and also supported by the
214 capacity of secretins to oligomerize outside the OM.
215 T2SS and T3SS secretins localization, assembly and OM insertion are mostly governed by their extreme
216 C-terminal S-domains reviewed by [53]. In the high-resolution structures, these S-domains form a helix-
217 turn-helix motif that extends laterally on the exterior of the β -barrel (Figure 1). This supports the notion
218 that S-domains have a key role in efficient secretin assembly and stability in addition to their pilotin-
219 binding function. S-domains are necessary and sufficient to ensure targeting and stabilization since the
220 graft of the PulD or InvG S-domains to the S-domain deficient FPE pIV secretin rendered the chimeras
221 functional, dependent on the PulS and InvH pilotins, respectively [54, 55]. S-domains of T2SS pilotin-
222 dependent secretins are formed by 2 α -helices, respectively involved in stabilization and pilotin
223 recognition. This structure-function relationship is confirmed by the absence of the second helix in
224 secretins targeting to the OM by an alternative pilotin-independent process [48], or for which no pilotin
225 has yet been identified. This is the case for XcpD of *P. aeruginosa* [26] for which, another mode of OM
226 targeting could be considered.

227

228 4.4. The periplasmic N-module composed of several successive N-domains

229 With the N3 RBM domain now considered part of the C-module, the secretin N-module is therefore
230 defined as the portion comprising all the domains N-terminal to the N3 RBM domain (Figure 1). Unlike
231 the C-module whose high-resolution structure allowed the precise positioning of each monomer up to
232 amino acids side chains, the lower resolution of N-modules does not allow a clear identification of the
233 monomers. In the majority of the available structures, the N-domains were only positioned by
234 homology-based building using monomeric crystal structures, thus often leading to steric clashes and
235 therefore questioning the accuracy of the models [9, 10, 26, 27, 30]. Such low resolution of N-modules
236 was systematically seen with the first isolated secretin structures, suggesting the requirement of
237 stabilizing partners, which was confirmed subsequently for complexes between secretins and their IM
238 partners [19, 56]. These structures indicate that the N-module is clearly dissociated from the C-module
239 through an unstructured density (Figure 1). This poorly resolved flexible zone may correspond to the
240 inter-domain region separating the OM-associated C-module and the periplasmic N-module. The
241 flexibility in the inter-domain region could allow for important structural rearrangements, essential for
242 the coexistence of the previously discussed different structural organization and stoichiometry
243 between the C- and N-modules.

244 All bacterial secretins harbour a N0 domain at their extreme N-terminus, which is involved in IM-
245 coupling. While N0 structure was not resolved in secretin oligomers, it has been determined for
246 monomeric truncated variants or oligomers in complex with their IM partners [22, 25, 27, 30, 57, 58].
247 N0 domains of T2SS, T4P, FPE and to some extent T3SS secretins have a similar structural organization,
248 thus suggesting a conserved packing arrangement among secretins. At the quaternary level, structures
249 obtained in combination with IM partners show that the N0 is oriented perpendicularly to the N-
250 domain above it (N1 for T2SS/T3SS, and N3 for T4P) [19, 56], while it is positioned in a parallel fashion
251 in absence of IM partners (Figure 1) [25, 58, 59]. N0 domains organization within secretin channels
252 appears to be highly variable even in term of stoichiometry. Inside a specific secretin family such as
253 T3SS, pentadecameric and hexadecameric organization have been proposed [22, 56]. For T2SS,
254 pentadecamers and dodecamers (hexamers of dimers), both physiologically relevant, were reported
255 [19, 25].

256 In addition to the conserved N0 domain, additional RBM domains are sometimes found between
257 N3 and N0. This is the case for T2SS and T3SS secretins N-modules, which display two RBMs (N1 and

258 N2) and one RBM (N1), respectively. These domains could define the size of the periplasmic chamber
259 therefore reflecting the nature of the envelope in which they are inserted. For example, in the
260 thermophilic bacterium *Thermus thermophilus*, the T4P secretin PilQ has an N-module composed of
261 five stacked rings, including four RBMs all dispensable for complex assembly but essential for function
262 [60]. This larger N-module could represent an adaptation to the thicker cell envelope of this bacterium.

263

264 4.5. Discovery of an optional top-gate (TG) in a sub-class of secretins

265 As new secretin structures were released (Table 1), common and specific determinants of the different
266 family members have emerged. This was the case for T2SS secretins, for which several structures
267 revealed the existence in the *Vibrio*-type subclass [61] of an additional apical domain called top-gate
268 (TG) or cap-gate (Figure 1) [10]. The TG has a conical structure formed by the convergence of 15 pairs
269 of antiparallel β -strands whose connecting loops are relatively loose, suggesting that the hairpin
270 formed by the TG is a dynamic structure alike the CG. The inner diameter of the TG defines a much
271 narrower opening compared to the large open-edged β -barrels formed by the other subclass lacking
272 TG and called *Klebsiella*-type (Figure 1). Given the directionality of effector transport in T2SS, the TG
273 should rotate outward to open and release the substrate in the extracellular medium. After substrate
274 release, the TG would return to its closed conformation to eventually start a new cycle. The presence
275 of such a structure at the top of some T2SS secretins could represent an additional gasket preventing
276 the entry of toxic molecules. Until now, no other type of secretins displayed obvious TG at their summit
277 (Figure 1 and Table 1), an observation consistent with the absence of a corresponding region in their
278 primary sequences [9].

279

280 **5. Concluding remarks**

281 Structural and functional study of bacterial secretins, which remained a mystery for more than 30
282 years, has largely benefited from the spectacular advances in structural biology and notably from the
283 breakthrough of cryo-EM. This revealed intriguing and sometimes unexpected quaternary features of
284 these giant gated double-barrelled channels – such as the interlacement and intertwining of unrelated
285 secondary and ternary structures of each monomer in gates, barrels or cages – providing a coherent
286 atomic quaternary picture. As we move towards a better mechanistic understanding of bacterial
287 secretins, several important challenges remain, including how secretins are transported, assembled
288 and inserted in the OM, how they open and close without compromising their remarkable stability.
289 We need to understand how these giant pores are motioned in the global secretion/assembly context
290 of their corresponding nanomachines, particularly for their poorly resolved N-terminal regions. The
291 ultimate goal – visualizing, at atomic scale, the secretins in their natural environment the bacterial
292 envelope – awaits a revolution in cryo-electron tomography allowing atomic resolution to be reached.

293

294 **Acknowledgements**

295 We would like to thank Dr. Martin Picard for the kind invitation to write this review in the frame of a
296 special issue covering the 2021 APPICOM GDR meeting. We are grateful to Dr Vladimir Pelicic and
297 members of the Voulhoux lab for careful reading of the manuscript, and fruitful discussions. T2SS
298 research in the Voulhoux lab is supported by the SYNERGY_T2SS ANR grant (ANR-19-CE11-0020-01).
299 B. Barbat is supported by a MESRI PhD studentship. B. Douzi research activity is supported by the
300 National Research Institute for Agriculture, Food and Environment (INRAE) and the Université de
301 Lorraine.

302

303 **Conflict of interest.**

304 None

305

306 **Contributions**

307 B. Barbat, B. Douzi and R. Voulhoux contributed to the design and the writing of the manuscript, B.
308 Barbat designed the figures and R. Voulhoux supervised the work.

309 **Figures & Table legends**

310 **Figure 1. Representative cryo-EM structures for each secretin type.** The PDB structures have been
311 scaled, aligned with the outer membrane (shaded orange rectangle), and colored according to the
312 following code. Red, monomer; gray, C-module (C+N3 domains); blue, N-module (N0±N1±N2
313 domains); green, S-domain; pink, PulS pilotin; orange, PulC IM-partner. **(Top)** Side view. The missing
314 N0 domain is represented by a shaded blue cylinder. The two different *Vibrio* (V) and *Klebsiella* (K)
315 types of T2SS secretins [61] are presented, as well as the “closed” (C) and “open” (O) states of the InvG
316 T3SS secretin. **(Bottom)** Cross-section view highlighting top-gate (TG) and central-gate (CG)
317 constrictions, as well as internal diameters. The disordered loops in N3 domains are indicated by *.
318 Dimensions (in Å) are from measurements on the PDB entries.

319 **Figure 2. Charge distribution of internal cavities in different secretin types.** The vertical cross-section
320 of the secretins presented in Figure 1, colored according to their inner surface charge using the APBS
321 Electrostatics Plug-in available in PyMol [29]. The color r scale is shown on the left. The position of N3
322 domains is indicated by a grey bar.

323 **Table 1. List of cryo-EM 3D structures of bacterial secretins at near-atomic resolution.** Secretins for
324 which a near-atomic resolution structure (<7Å) has been published is listed. For each structure, the
325 name of the secretin and its organism of origin, its PDB entry, the stoichiometry, domains that are
326 resolved and the overall resolution are indicated. When useful, additional information on specific
327 features of the structure is provided.

328

329 **References**

- 330 [1] C. d'Enfert, I. Reyss, C. Wandersman, A.P. Pugsley, Protein secretion by gram-negative bacteria.
331 Characterization of two membrane proteins required for pullulanase secretion by *Escherichia coli*
332 K-12, J Biol Chem, 264 (1989) 17462-17468.
- 333 [2] D.D. Majewski, L.J. Worrall, N.C. Strynadka, Secretins revealed: structural insights into the giant
334 gated outer membrane portals of bacteria, Curr Opin Struct Biol, 51 (2018) 61-72.
- 335 [3] W. Bitter, M. Koster, M. Latijnhouwers, H. de Cock, J. Tommassen, Formation of oligomeric rings by
336 XcpQ and PilQ, which are involved in protein transport across the outer membrane of
337 *Pseudomonas aeruginosa*, Mol Microbiol, 27 (1998) 209-219.
- 338 [4] K.R. Hardie, S. Lory, A.P. Pugsley, Insertion of an outer membrane protein in *Escherichia coli* requires
339 a chaperone-like protein, EMBO J, 15 (1996) 978-988.
- 340 [5] B.I. Kazmierczak, D.L. Mielke, M. Russel, P. Model, pIV, a filamentous phage protein that mediates
341 phage export across the bacterial cell envelope, forms a multimer, J Mol Biol, 238 (1994) 187-198.
- 342 [6] M. Koster, W. Bitter, H. de Cock, A. Allaoui, G.R. Cornelis, J. Tommassen, The outer membrane
343 component, YscC, of the Yop secretion machinery of *Yersinia enterocolitica* forms a ring-shaped
344 multimeric complex, Mol Microbiol, 26 (1997) 789-797.
- 345 [7] N. Nouwen, N. Ranson, H. Saibil, B. Wolpensinger, A. Engel, A. Ghazi, A.P. Pugsley, Secretin PulD:
346 association with pilot PulS, structure, and ion-conducting channel formation, Proc Natl Acad Sci U
347 S A, 96 (1999) 8173-8177.
- 348 [8] N. Opalka, R. Beckmann, N. Boisset, M.N. Simon, M. Russel, S.A. Darst, Structure of the filamentous
349 phage pIV multimer by cryo-electron microscopy, J Mol Biol, 325 (2003) 461-470.

- 350 [9] L.J. Worrall, C. Hong, M. Vuckovic, W. Deng, J.R. Bergeron, D.D. Majewski, R.K. Huang, T. Spreter,
351 B.B. Finlay, Z. Yu, N.C. Strynadka, Near-atomic-resolution cryo-EM analysis of the *Salmonella* T3S
352 injectisome basal body, *Nature*, 540 (2016) 597-601.
- 353 [10] Z. Yan, M. Yin, D. Xu, Y. Zhu, X. Li, Structural insights into the secretin translocation channel in the
354 type II secretion system, *Nat Struct Mol Biol*, 24 (2017) 177-183.
- 355 [11] S. Genin, C.A. Boucher, A superfamily of proteins involved in different secretion pathways in gram-
356 negative bacteria: modular structure and specificity of the N-terminal domain, *Mol Gen Genet*, 243
357 (1994) 112-118.
- 358 [12] L. Horvathova, V. Zarsky, T. Panek, R. Derelle, J. Pyrih, A. Motyckova, V. Klapstova, M. Vinopalova,
359 L. Markova, L. Voleman, V. Klimes, M. Petru, Z. Vaitova, I. Cepicka, K. Hryzakova, K. Harant, M.W.
360 Gray, M. Chami, I. Guilvout, O. Francetic, B. Franz Lang, C. Vlcek, A.D. Tsaousis, M. Elias, P. Dolezal,
361 Analysis of diverse eukaryotes suggests the existence of an ancestral mitochondrial apparatus
362 derived from the bacterial type II secretion system, *Nat Commun*, 12 (2021) 2947.
- 363 [13] R. Brok, P. Van Gelder, M. Winterhalter, U. Ziese, A.J. Koster, H. de Cock, M. Koster, J. Tommassen,
364 W. Bitter, The C-terminal domain of the *Pseudomonas* secretin XcpQ forms oligomeric rings with
365 pore activity, *J Mol Biol*, 294 (1999) 1169-1179.
- 366 [14] K.V. Korotkov, T. Gonen, W.G. Hol, Secretins: dynamic channels for protein transport across
367 membranes, *Trends Biochem Sci*, 36 (2011) 433-443.
- 368 [15] K.V. Korotkov, E. Pardon, J. Steyaert, W.G. Hol, Crystal structure of the N-terminal domain of the
369 secretin GspD from ETEC determined with the assistance of a nanobody, *Structure*, 17 (2009) 255-
370 265.
- 371 [16] D. Ghosal, K.W. Kim, H. Zheng, M. Kaplan, H.K. Truchan, A.E. Lopez, I.E. McIntire, J.P. Vogel, N.P.
372 Cianciotto, G.J. Jensen, *In vivo* structure of the *Legionella* type II secretion system by electron
373 cryotomography, *Nat Microbiol*, 4 (2019) 2101-2108.
- 374 [17] T.L. Leighton, N. Dayalani, L.M. Sampaleanu, P.L. Howell, L.L. Burrows, Novel Role for PilNO in Type
375 IV Pilus Retraction Revealed by Alignment Subcomplex Mutations, *J Bacteriol*, 197 (2015) 2229-
376 2238.
- 377 [18] N. Bayan, I. Guilvout, A.P. Pugsley, Secretins take shape, *Mol Microbiol*, 60 (2006) 1-4.
- 378 [19] A.A. Chernyatina, H.H. Low, Core architecture of a bacterial type II secretion system, *Nat Commun*,
379 10 (2019) 5437.
- 380 [20] M. Chami, I. Guilvout, M. Gregorini, H.W. Remigy, S.A. Muller, M. Valerio, A. Engel, A.P. Pugsley,
381 N. Bayan, Structural insights into the secretin PulD and its trypsin-resistant core, *J Biol Chem*, 280
382 (2005) 37732-37741.
- 383 [21] M. McCallum, S. Tammam, J.L. Rubinstein, L.L. Burrows, P.L. Howell, CryoEM map of *Pseudomonas*
384 *aeruginosa* PilQ enables structural characterization of TsaP, *Structure*, 29 (2021) 457-466 e454.
- 385 [22] J. Hu, L.J. Worrall, C. Hong, M. Vuckovic, C.E. Atkinson, N. Caveney, Z. Yu, N.C.J. Strynadka, Cryo-
386 EM analysis of the T3S injectisome reveals the structure of the needle and open secretin, *Nat*
387 *Commun*, 9 (2018) 3840.
- 388 [23] M. Lunelli, A. Kamprad, J. Burger, T. Mielke, C.M.T. Spahn, M. Kolbe, Cryo-EM structure of the
389 *Shigella* type III needle complex, *PLoS Pathog*, 16 (2020) e1008263.
- 390 [24] S. Miletic, D. Fahrenkamp, N. Goessweiner-Mohr, J. Wald, M. Pantel, O. Vesper, V. Kotov, T.C.
391 Marlovits, Substrate-engaged type III secretion system structures reveal gating mechanism for
392 unfolded protein translocation, *Nat Commun*, 12 (2021) 1546.
- 393 [25] B. Douzi, N.T.T. Trinh, S. Michel-Souzy, A. Desmyter, G. Ball, P. Barbier, A. Kosta, E. Durand, K.T.
394 Forest, C. Cambillau, A. Roussel, R. Voulhoux, Unraveling the Self-Assembly of the *Pseudomonas*
395 *aeruginosa* XcpQ Secretin Periplasmic Domain Provides New Molecular Insights into Type II
396 Secretion System Secretin Architecture and Dynamics, *MBio*, 8(5) (2017) e01185-17.
- 397 [26] I.D. Hay, M.J. Belousoff, T. Lithgow, Structural Basis of Type 2 Secretion System Engagement
398 between the Inner and Outer Bacterial Membranes, *MBio*, 8(5) (2017) e01344-17.
- 399 [27] R. Conners, M. McLaren, U. Lapinska, K. Sanders, M.R.L. Stone, M.A.T. Blaskovich, S. Pagliara, B.
400 Daum, J. Rakonjac, V.A.M. Gold, CryoEM structure of the outer membrane secretin channel pIV
401 from the f1 filamentous bacteriophage, *Nat Commun*, 12 (2021) 6316.

- 402 [28] I.D. Hay, M.J. Belousoff, R.A. Dunstan, R.S. Bamert, T. Lithgow, Structure and Membrane
403 Topography of the Vibrio-Type Secretin Complex from the Type 2 Secretion System of
404 Enteropathogenic *Escherichia coli*, *J Bacteriol*, 200 (2018) e00521-17.
- 405 [29] E. Jurrus, D. Engel, K. Star, K. Monson, J. Brandi, L.E. Felberg, D.H. Brookes, L. Wilson, J. Chen, K.
406 Liles, M. Chun, P. Li, D.W. Gohara, T. Dolinsky, R. Konecny, D.R. Koes, J.E. Nielsen, T. Head-Gordon,
407 W. Geng, R. Krasny, G.W. Wei, M.J. Holst, J.A. McCammon, N.A. Baker, Improvements to the APBS
408 biomolecular solvation software suite, *Protein Sci*, 27 (2018) 112-128.
- 409 [30] S.J. Weaver, D.R. Ortega, M.H. Sazinsky, T.N. Dalia, A.B. Dalia, G.J. Jensen, CryoEM structure of the
410 type IVa pilus secretin required for natural competence in *Vibrio cholerae*, *Nat Commun*, 11 (2020)
411 5080.
- 412 [31] T.C. Marlovits, T. Kubori, A. Sukhan, D.R. Thomas, J.E. Galan, V.M. Unger, Structural insights into
413 the assembly of the type III secretion needle complex, *Science*, 306 (2004) 1040-1042.
- 414 [32] P. Burghout, R. van Boxtel, P. Van Gelder, P. Ringler, S.A. Muller, J. Tommassen, M. Koster,
415 Structure and electrophysiological properties of the YscC secretin from the type III secretion
416 system of *Yersinia enterocolitica*, *J Bacteriol*, 186 (2004) 4645-4654.
- 417 [33] E. Disconzi, I. Guilvout, M. Chami, M. Masi, G.H. Huysmans, A.P. Pugsley, N. Bayan, Bacterial
418 secretins form constitutively open pores akin to general porins, *J Bacteriol*, 196 (2014) 121-128.
- 419 [34] J. Spagnuolo, N. Opalka, W.X. Wen, D. Gagic, E. Chabaud, P. Bellini, M.D. Bennett, G.E. Norris, S.A.
420 Darst, M. Russel, J. Rakonjac, Identification of the gate regions in the primary structure of the
421 secretin pIV, *Mol Microbiol*, 76 (2010) 133-150.
- 422 [35] I. Guilvout, M. Chami, C. Berrier, A. Ghazi, A. Engel, A.P. Pugsley, N. Bayan, In vitro multimerization
423 and membrane insertion of bacterial outer membrane secretin PulD, *J Mol Biol*, 382 (2008) 13-23.
- 424 [36] T. Spreter, C.K. Yip, S. Sanowar, I. Andre, T.G. Kimbrough, M. Vuckovic, R.A. Pfuetzner, W. Deng,
425 A.C. Yu, B.B. Finlay, D. Baker, S.I. Miller, N.C. Strynadka, A conserved structural motif mediates
426 formation of the periplasmic rings in the type III secretion system, *Nat Struct Mol Biol*, 16 (2009)
427 468-476.
- 428 [37] J.R.C. Bergeron, L.J. Worrall, S. De, N.G. Sgourakis, A.H. Cheung, E. Lameignere, M. Okon, G.A.
429 Wasney, D. Baker, L.P. McIntosh, N.C.J. Strynadka, The modular structure of the inner-membrane
430 ring component PrgK facilitates assembly of the type III secretion system basal body, *Structure*, 23
431 (2015) 161-172.
- 432 [38] N. Zeytuni, C. Hong, K.A. Flanagan, L.J. Worrall, K.A. Theiltges, M. Vuckovic, R.K. Huang, S.C.
433 Massoni, A.H. Camp, Z. Yu, N.C. Strynadka, Near-atomic resolution cryoelectron microscopy
434 structure of the 30-fold homooligomeric SpoIIAG channel essential to spore formation in *Bacillus*
435 *subtilis*, *Proc Natl Acad Sci U S A*, 114 (2017) E7073-E7081.
- 436 [39] G.H. Huysmans, Folding outer membrane proteins independently of the beta-barrel assembly
437 machinery: an assembly pathway for multimeric complexes?, *Biochem Soc Trans*, 44 (2016) 845-
438 850.
- 439 [40] B. Liu, H. Chan, E. Bauda, C. Contreras-Martel, L. Bellard, A.M. Villard, C. Mas, E. Neumann, D.
440 Fenel, A. Favier, M. Serrano, A.O. Henriques, C.D.A. Rodrigues, C. Morlot, Structural insights into
441 ring-building motif domains involved in bacterial sporulation, *J Struct Biol*, 214 (2022) 107813.
- 442 [41] J. Koo, L.L. Burrows, P.L. Howell, Decoding the roles of pilotins and accessory proteins in secretin
443 escort services, *FEMS Microbiol Lett*, 328 (2012) 1-12.
- 444 [42] P. Burghout, F. Beckers, E. de Wit, R. van Boxtel, G.R. Cornelis, J. Tommassen, M. Koster, Role of
445 the pilot protein YscW in the biogenesis of the YscC secretin in *Yersinia enterocolitica*, *J Bacteriol*,
446 186 (2004) 5366-5375.
- 447 [43] I. Guilvout, M. Chami, A. Engel, A.P. Pugsley, N. Bayan, Bacterial outer membrane secretin PulD
448 assembles and inserts into the inner membrane in the absence of its pilotin, *EMBO J*, 25 (2006)
449 5241-5249.
- 450 [44] J. Natarajan, N. Singh, D. Rapaport, Assembly and targeting of secretins in the bacterial outer
451 membrane, *Int J Med Microbiol*, 309 (2019) 151322.

- 452 [45] S. Collin, I. Guilvout, N.N. Nickerson, A.P. Pugsley, Sorting of an integral outer membrane protein
453 via the lipoprotein-specific Lol pathway and a dedicated lipoprotein pilotin, *Mol Microbiol*, 80
454 (2011) 655-665.
- 455 [46] S. Collin, I. Guilvout, M. Chami, A.P. Pugsley, YaeT-independent multimerization and outer
456 membrane association of secretin PulD, *Mol Microbiol*, 64 (2007) 1350-1357.
- 457 [47] R. Voulhoux, M.P. Bos, J. Geurtsen, M. Mols, J. Tommassen, Role of a highly conserved bacterial
458 protein in outer membrane protein assembly, *Science*, 299 (2003) 262-265.
- 459 [48] S.P. Howard, L.F. Estrozi, Q. Bertrand, C. Contreras-Martel, T. Strozen, V. Job, A. Martins, D. Fenel,
460 G. Schoehn, A. Dessen, Structure and assembly of pilotin-dependent and -independent secretins
461 of the type II secretion system, *PLoS Pathog*, 15 (2019) e1007731.
- 462 [49] V. Viarre, E. Cascales, G. Ball, G.P. Michel, A. Filloux, R. Voulhoux, HxcQ liposecretin is self-piloted
463 to the outer membrane by its N-terminal lipid anchor, *J Biol Chem*, 284 (2009) 33815-33823.
- 464 [50] H.D. Bernstein, Looks can be deceiving: recent insights into the mechanism of protein secretion
465 by the autotransporter pathway, *Mol Microbiol*, 97 (2015) 205-215.
- 466 [51] M.A. Dunstone, R.K. Tweten, Packing a punch: the mechanism of pore formation by cholesterol
467 dependent cytolysins and membrane attack complex/perforin-like proteins, *Curr Opin Struct Biol*,
468 22 (2012) 342-349.
- 469 [52] S.J. Tilley, H.R. Saibil, The mechanism of pore formation by bacterial toxins, *Curr Opin Struct Biol*,
470 16 (2006) 230-236.
- 471 [53] Y.R.O. Silva, C. Contreras-Martel, P. Macheboeuf, A. Dessen, Bacterial secretins: Mechanisms of
472 assembly and membrane targeting, *Protein Sci*, 29 (2020) 893-904.
- 473 [54] S. Daefler, M. Russel, The *Salmonella typhimurium* InvH protein is an outer membrane lipoprotein
474 required for the proper localization of InvG, *Mol Microbiol*, 28 (1998) 1367-1380.
- 475 [55] S. Daefler, M. Russel, P. Model, Module swaps between related translocator proteins pIV(f1),
476 pIV(IKe) and PulD: identification of a specificity domain, *J Mol Biol*, 266 (1997) 978-992
- 477 [56] J. Hu, L.J. Worrall, M. Vuckovic, C. Hong, W. Deng, C.E. Atkinson, B. Brett Finlay, Z. Yu, N.C.J.
478 Strynadka, T3S injectisome needle complex structures in four distinct states reveal the basis of
479 membrane coupling and assembly, *Nat Microbiol*, 4 (2019) 2010-2019.
- 480 [57] K.V. Korotkov, T.L. Johnson, M.G. Jobling, J. Pruneda, E. Pardon, A. Heroux, S. Turley, J. Steyaert,
481 R.K. Holmes, M. Sandkvist, W.G. Hol, Structural and functional studies on the interaction of GspC
482 and GspD in the type II secretion system, *PLoS Pathog*, 7 (2011) e1002228.
- 483 [58] R. Van der Meeren, Y. Wen, P. Van Gelder, J. Tommassen, B. Devreese, S.N. Savvides, New insights
484 into the assembly of bacterial secretins: structural studies of the periplasmic domain of XcpQ from
485 *Pseudomonas aeruginosa*, *J Biol Chem*, 288 (2013) 1214-1225.
- 486 [59] K.V. Korotkov, J.R. Delarosa, W.G.J. Hol, A dodecameric ring-like structure of the N0 domain of the
487 type II secretin from enterotoxigenic *Escherichia coli*, *J Struct Biol*, 183 (2013) 354-362.
- 488 [60] R. Salzer, E. D'Imprima, V.A. Gold, I. Rose, M. Drechsler, J. Vonck, B. Averhoff, Topology and
489 Structure/Function Correlation of Ring- and Gate-forming Domains in the Dynamic Secretin
490 Complex of *Thermus thermophilus*, *J Biol Chem*, 291 (2016) 14448-14456.
- 491 [61] R.A. Dunstan, E. Heinz, L.C. Wijeyewickrema, R.N. Pike, A.W. Purcell, T.J. Evans, J. Praszkiel, R.M.
492 Robins-Browne, R.A. Strugnell, K.V. Korotkov, T. Lithgow, Assembly of the type II secretion system
493 such as found in *Vibrio cholerae* depends on the novel Pilotin AspS, *PLoS Pathog*, 9 (2013)
494 e1003117.
- 495 [62] M. Yin, Z. Yan, X. Li, Structural insight into the assembly of the type II secretion system pilotin-
496 secretin complex from enterotoxigenic *Escherichia coli*, *Nat Microbiol*, 3 (2018) 581-587.

System	PDB entry	Secretin name	Organism	Domains	Resolution	Secretin's Stoichiometry	Remarks (in complex with)	Reference
T2SS	5WLN	XcpD	<i>P. aeruginosa</i>	S/C/N3/N2	3.57 Å	15		[26]
	6I1X	ExeD	<i>A. hydrophila</i>	S/C/N3/N2/N1	3.7 Å	15		[48]
	5W68	GspD	<i>E. coli EPEC</i>	S/C/N3	3.3 Å	15	Top Gate	[28]
	5ZDH	GspD	<i>E. coli ETEC</i>	S/C/N3/N2/N1	3.2 Å	15	Top Gate (AspS)	[62]
	5WQ7	GspD	<i>E. coli K12</i>	S/C/N3/N2/N1	3.04 Å	15 & 16		[10]
	5WQ8	GspD	<i>V. cholerae</i>	S/C/N3/N2/N1	3.26 Å	15	Top Gate	[10]
	5WQ9	GspD _{G453A}	<i>V. cholerae</i>	S/C/N3/N2/N1	4.22 Å	15	Partially open state	[10]
	6I1Y	EpsD	<i>V. vulnificus</i>	S/C/N3/N2/N1	3.4 Å	15	Top gate	[48]
	6HCG	PulD	<i>K. pneumoniae</i>	S/C/N3/N2/N1/N0	4.3 Å	15	(PulCS)	[19]
T3SS	6DV3	InvG	<i>S. enterica</i>	S/C/N3/N1/N0	4.1 Å	15	Open state	[22]
	6DV6	InvG	<i>S. enterica</i>	S/C/N3	3.9 Å	15	Open state	[22]
	6PEE	InvG	<i>S. enterica</i>	S/C/N3	3.42 Å	15		[56]
	6PEP	InvG	<i>S. enterica</i>	N1/N0	3.8 Å	16	(SpaPQR:PrgHIJ)	[56]
	6PEM	InvG	<i>S. enterica</i>	N1/N0	3.5 Å	16	(SpaPQR:PrgHK)	[56]
	6Q14	InvG	<i>S. enterica</i>	S/C/N3/N1/N0	3.8 Å	15 (S/C/N3) 16 (N1/N0)	(SpaPQR:PrgHK)	[56]
	6Q15	InvG	<i>S. enterica</i>	S/C/N3/N1/N0	5.15 Å	15 (S/C/N3) 16 (N1/N0)	Open state (SpaPQR:PrgHIJK)	[56]
	6Q16	InvG	<i>S. enterica</i>	N1/N0	4.1 Å	16	(SpaPQR:PrgHIJK)	[56]
	5TCQ	InvG	<i>S. enterica</i>	S/C/N3	3.6 Å	15		[9]
	5TCR	InvG	<i>S. enterica</i>	S/C/N3/N1/N0	6.3 Å	15	(PrgHK)	[9]
	7AHI	InvG	<i>S. enterica</i>	S/C/N3/N1/N0	3.3 Å	15 (S/C/N3) 16 (N1/N0)	(SpaPQR:PrgHIJK: SptP)	[24]
	7AH9	InvG	<i>S. enterica</i>	S/C/N3/N1/N0	3.3 Å	15 (S/C/N3) 16 (N1/N0)	(SpaPQR:PrgHIJK: SptP)	[24]
	6RWK	MxiD	<i>S. flexneri</i>	N1/N0	3.86 Å	16	(MxiG)	[23]
T4P	6VE2	PilQ	<i>P. aeruginosa</i>	C/N3	4.3 Å	14	(TsaP)	[21]
	6VE3	PilQ	<i>P. aeruginosa</i>	C/N3	4.3 Å	14		[21]
	6VE4	PilQ	<i>P. aeruginosa</i>	C/N3	6.9 Å	15		[21]
	6W6M	PilQ	<i>V. cholerae</i>	C/N3/N0	2.7 Å	14		[30]
FPE	7OFH	pIV	F1 filamentous bacteriophage	C/N3	2.7 Å	15		[27]

Table1

Secretins for which a near-atomic resolution structure (<7Å) has been published is listed. For each structure, the name of the secretin and its organism of origin, its PDB entry, the stoichiometry, domains that are resolved and the overall resolution are indicated. When useful, additional information on specific features of the structure is provided.

Figure 1

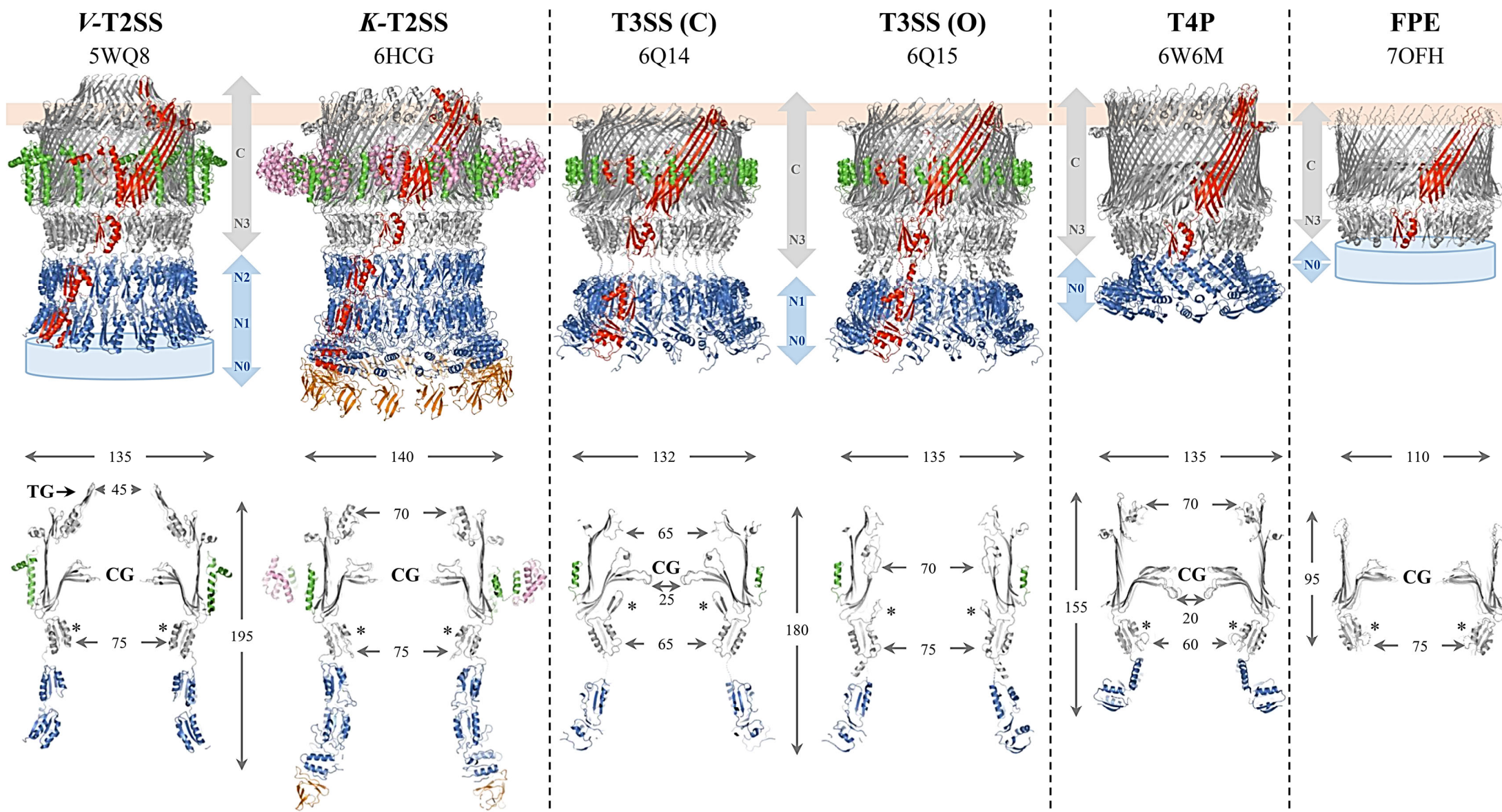


Figure 2

